

Long GRBs observations up to subTeV energies: sources inhomogeneity



I. V. Arkhangelskaja, A. E. Sukhov, D. S. Gorbunov, K. S. Chelidze
National Research Nuclear University MEPhI, Moscow, Russia
e-mail: irene.belousova@usa.net

1. Introduction: short, long and intermediate GRBs

Several thousands of GRBs were observed by various experiments, but their sources of origin still remain unclear up to now. The first database with sufficient to event duration analysis volume was made on data of the Compton Gamma Ray Observatory (CGRO) in 1991 - see, for example, [1]. Four experiments onboard CGRO: BATSE, OSSE, COMPTEL and EGRET [2] provided the widest energy range since of 10 keV up to more than 20 GeV. GRBs duration characterized by t_{90} and t_{50} accordingly to BATSE data analysis [3, 4]. These 2 parameters are the times for 90% and 50% of burst statistics (i.e. intervals where the accumulation integrated burst's counts raise from 5% to 95% and for 25% to 75% correspondingly). Two bursts classes' existence had shown on GRBs on t_{90} distribution analysis: long and short GRBs separated by $t_{90} \approx 2$ s [4].

The subgroup of intermediate GRBs was first found in 1997 [5] during 4B current BATSE catalogue [6] analysis at 99% confidence level in duration interval of $0.8 \text{ s} \leq t_{90} \leq 50 \text{ s}$ with $\langle t_{90} \rangle \approx 3$ s taking into account duration and duration-hardness distributions. Additional criterion of burst spectrum description was hardness H_{32} , introduced using BATSE data analysis results. It was defined as the ratio of fluence in third and second energy channels. Taking into account duration-hardness distributions analysis the following criteria were obtained for short ($t_{90} < 3$ s, $\langle t_{90} \rangle \approx 0.5$ s, $H_{32} > 6.00$) and long ($t_{90} > 5$ s, $\langle t_{90} \rangle \approx 30$ s, $H_{32} < 1.85$) GRBs. Figure 1 presents this subgroup appearance in BATSE data.

Now there are two satellite experiments which database volumes are sufficient to burst duration analysis: Fermi and Swift. There are 2 instruments allows GRB registration onboard Fermi gamma-ray observatory [7]: GBM [8] and (LAT) [9]. It operate since

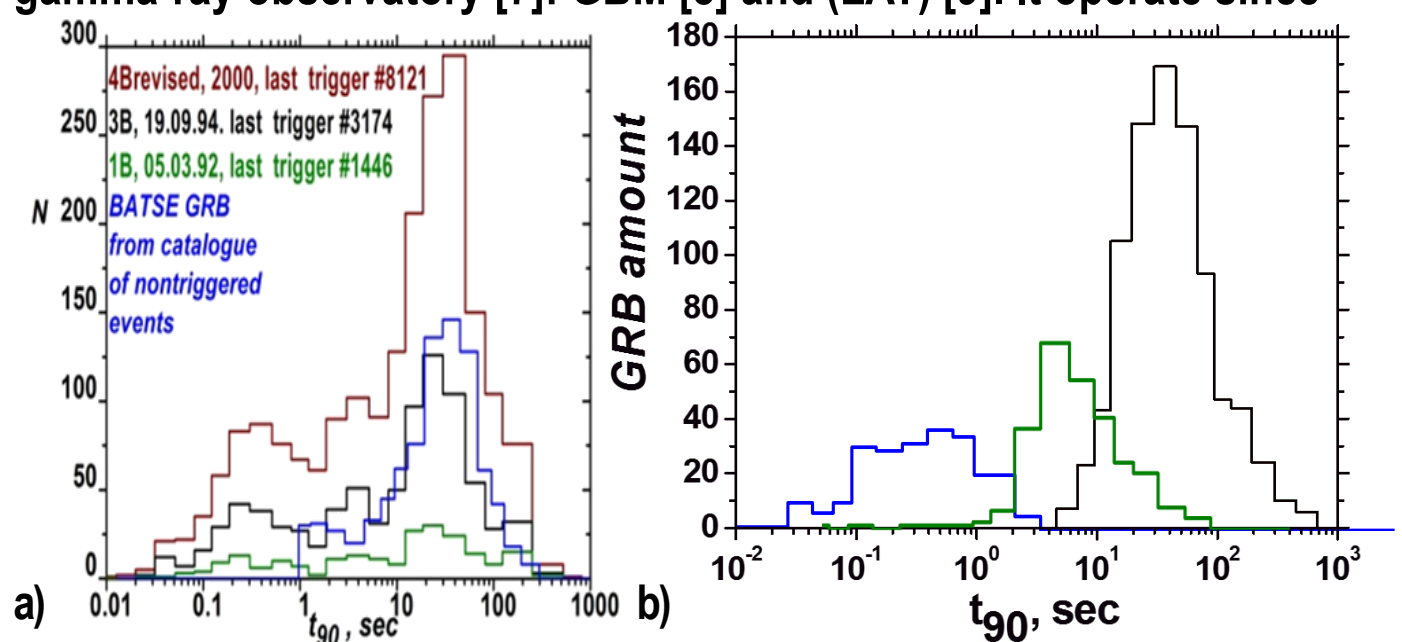


Fig. 1. Intermediate GRBs subgroup appearance on BATSE data: (a) in duration distributions for 1B, 3B and 4B revised catalogues and its absence in non-triggered event catalogue; (b) in duration distributions obtained after using additional criteria defined due hardness analysis.

2008 July and now 2595 GRBs identified since using GBM [10] and more than 148 GRBs using LAT [11, 12]. Three bursts detectors located onboard Swift Observatory [13]: BAT, XRT and UVOT. BAT is a highly sensitive coded aperture imaging instrument designed to provide GRBs observations with large field of view (1.4 steradian half coded) and 4-arcmin positions definition in energy bands 15-150 keV for imaging mode and up to 500 keV with a non-coded response. It was launched November 20, 2004 [13]. The XRT is a CCD imaging spectrometer at the focal plane of a 3.5 m focal length, an energy range of 0.2 - 10 keV with a 23x23 square arcmin FOV. The UVOT is an optical and UV 30-cm aperture telescope operating over a range of 170-650 nm with a 17x17 square arcmin FOV. Current GRBs catalogue published due to BAT data analysis. contains ~ 1300 bursts [14].

Unfortunately, duration of registered event strongly depends on detector energy band and method used for temporal profile analysis - see, for example, [15]. These reasons lead the same events could have different duration on data of various detectors. For example, GRB190114C (18:39:48 UT) had $t_{90} = 361.5 \pm 11.7$ s in energy range 15-350 keV on Swift/BAT data [14, 17] but $t_{90} = 116 \pm 1$ s in energy band 50-300 keV on Fermi/GBM data [10, 18]. Thus, each experiment subset needs separately duration analysis [15, 16].

Because of sufficient amount of GRBs located at high redshift (see redshift corresponding columns in catalogues [11, 12, 14]) its sources' origins nature is cosmological. Therefore correction to cosmological dilation of GRBs duration should be consider because of real cosmological sources time properties should be investigated only taking into account its redshift. Unfortunately several LAT GRBs weren't registered by GBM and information about its duration is absent. LAT GRBs distribution on burst duration t_{90} and cosmologically corrected

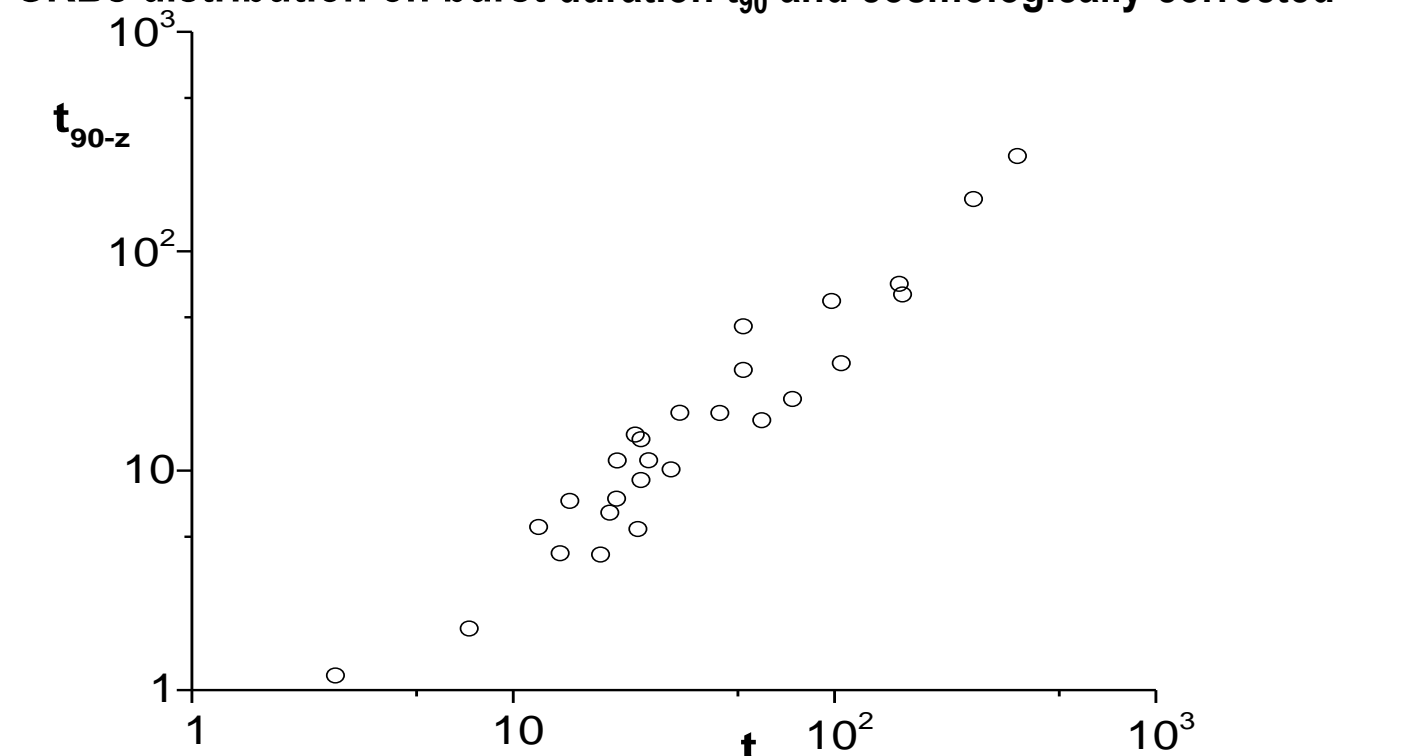


Fig. 2. GRBs distribution on burst duration t_{90} and cosmologically corrected $t_{90,z}$ is presented at figure 2. Of course, several correlations exist between burst duration and this value with cosmological correction, but it is impossible to make any conclusions without information just about distance to burst. Thus, bursts duration distributions should analyzed only taking into account cosmological correction. Duration distributions without and with correction to cosmological dilation for GRB from BAT catalogue are shown at figure 3. Results of analysis allow concluding appearance of burst subgroup similar to BATSE intermediate GRBs.

2. High energy gamma-emission during GRBs

During several GRBs very high-energy photons were detected both in

Several thousands of GRBs were observed by various experiments, but their sources of origin still remain unclear up to now. During several GRBs very high-energy photons were detected both in space and ground-based experiments (up to some tens of GeV and up to some TeV, respectively). For example, GRB 190114C was detected by Fermi and MAGIC in very wide band up to subTeV energies. 18 photons were observed by Milagro in energy band 0.1-10 TeV within 190 interval during GRB 970417a. Redshift measurements allow analyzing additional parameter and at least two long GRBs subgroup were separated with different characteristic distances $z \sim 1.1$ and $z \sim 2.2$. Here we introduce new value Rt is ratio of maximum energy photon arrival time to burst duration and it not required cosmological correction. At least 2 groups of long GRBs could be separated using Rt : for 14 events highest energy gammas detected within t_{90} interval, but for other 41 bursts it registered more than 10 seconds later than one. Moreover, preliminary results of analysis allow concluding three types of GRBs with high energy emission registration without dependence of burst duration value. During first subtype events high energy emission duration interval smaller than t_{90} . Second subtype characterized longer period of HE emission than t_{90} . But second subtype bursts divided to 2 subgroups. For one (a) γ with E_{max} arrived within t_{90} , for other such γ was registered later than t_{90} . Thus, preliminary analysis results allow conclude long GRBs population inhomogeneity.

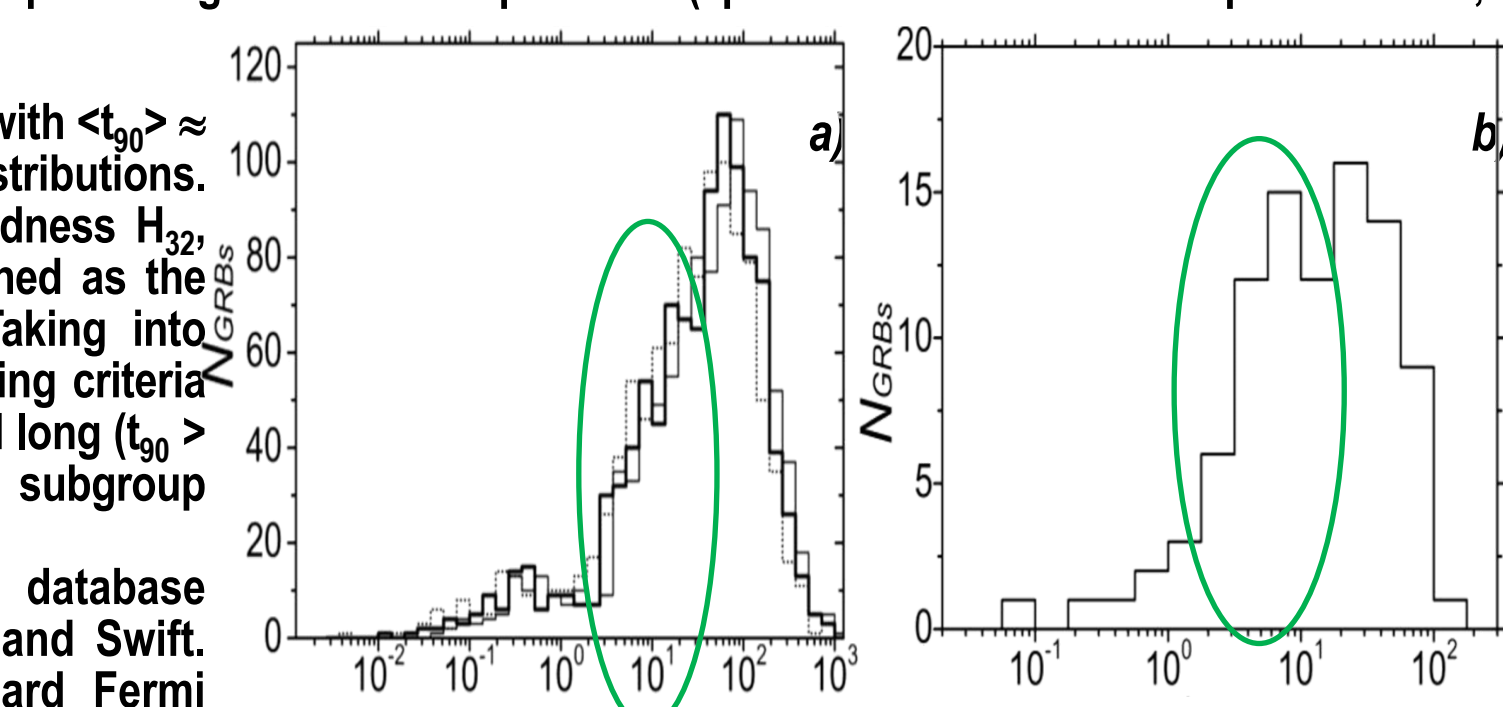


Fig. 3. Results of analysis of GRB from BAT catalogue: duration distribution without (a) and with (b) correction to cosmological dilation respectively). Gamma-quanta with energies $E_{\gamma} > 20$ MeV were first registered during GRB in satellite experiment onboard the CGRO in 1991 [19]. 18 photons were observed by Milagro in region 0.1-10 TeV within t_{90} interval during GRB 970417a [20]. Now GRB high energy γ -emission was observed both during short and long bursts, but photons in band $E > 0.1$ TeV usually observed only during long GRBs. Usually high energy γ -emission during long GRBs registered some

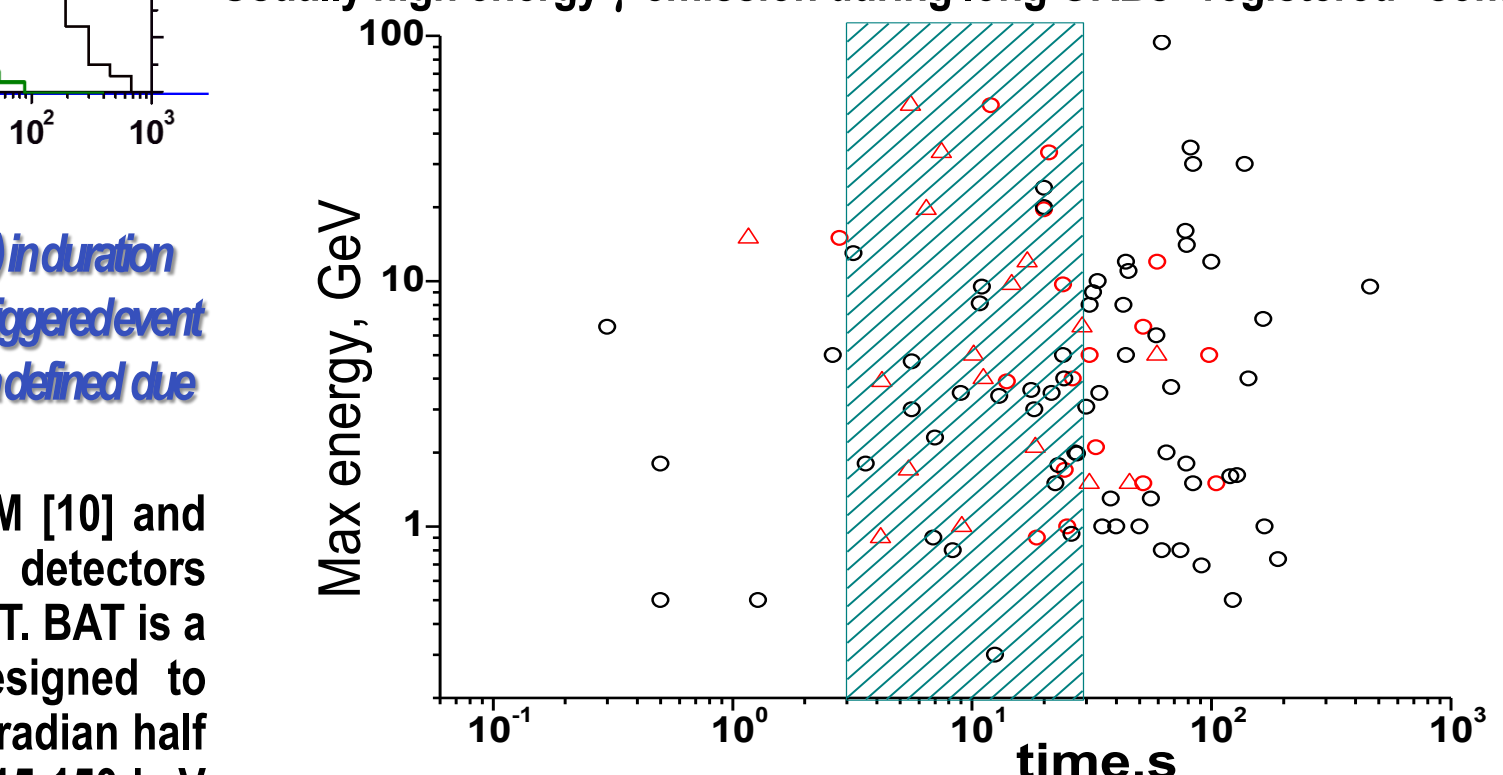


Fig. 4. LAT GRBs distribution on burst duration and maximum registered energy (circles). Red circles shows events with known redshift and red triangles represent these burst duration t_{90} after cosmological correction. Dashed region indicate associated intermediate GRBs area on results of fig.3 analysis

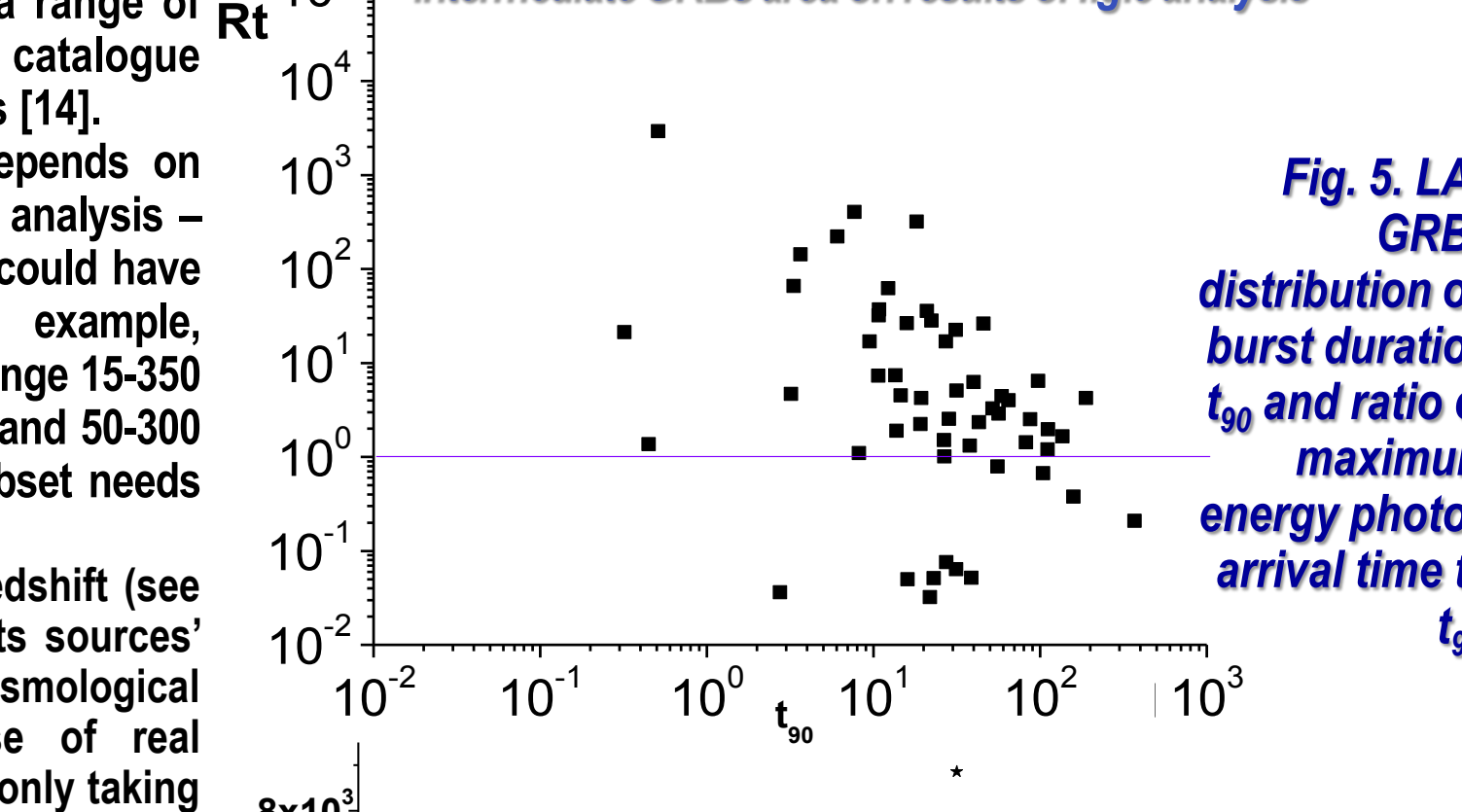


Fig. 5. LAT GRBs distribution on burst duration t_{90} and ratio of maximum energy photon arrival time to t_{90} .

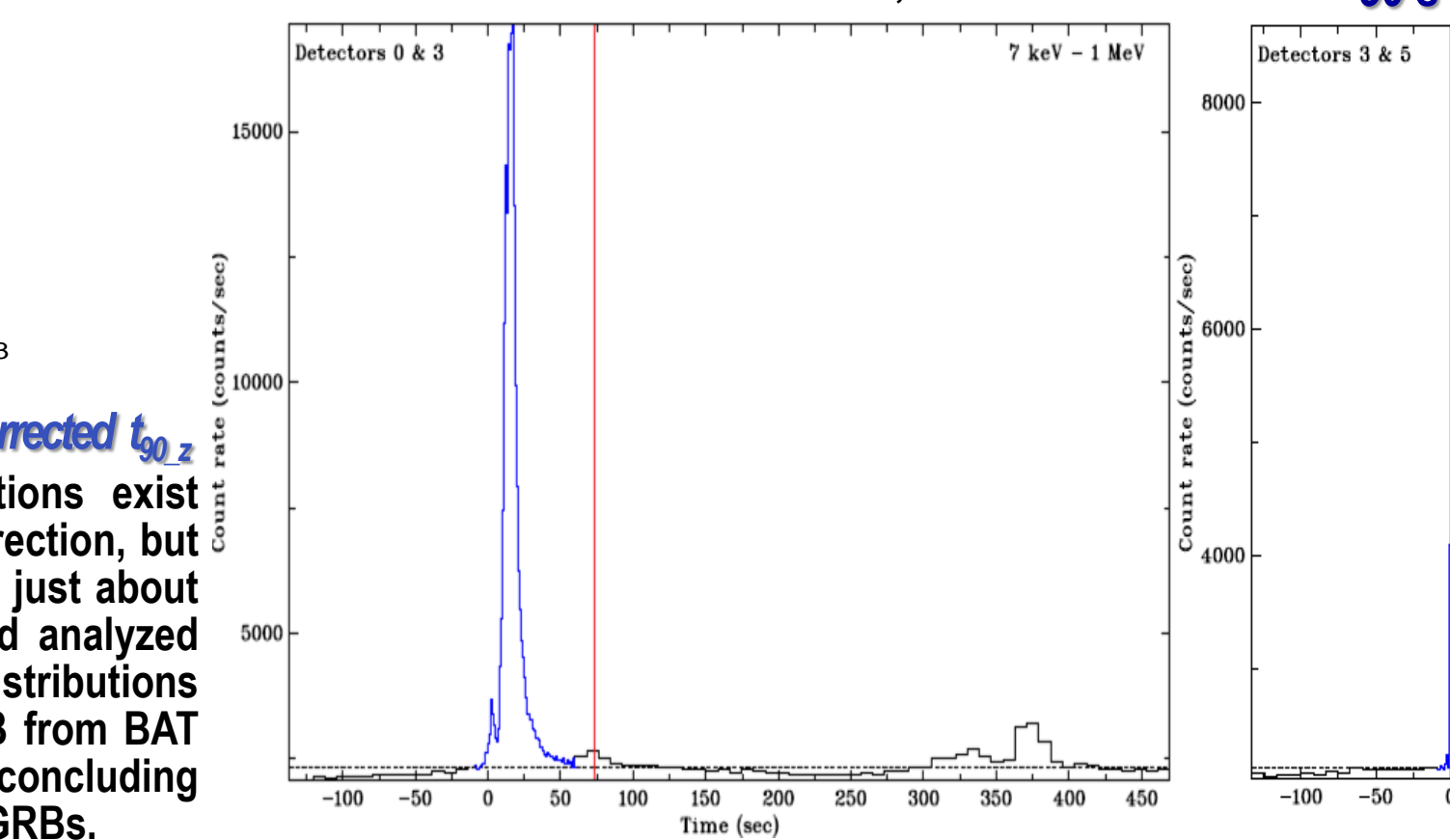


Fig. 7. The examples of low energy temporal profiles on GBM data for GRBs with different properties of Rt : a) GRB160509374 - subgroup 2a, b) GRB141222298 - subgroup 1, c) GRB131018673 - subgroup 1b. Red vertical line indicate arrival time for gamma-quantum with maximum energy

It is seen that after cosmological correction bursts with maximum registered energy mostly shifted to region correspond on event duration to intermediate GRBs. Unfortunately only 55 LAT GRBs has information both about redshifts and t_{90} .

For next analysis we introduce new value Rt is ratio of maximum energy photon arrival time to burst duration and this value not required cosmological correction. The distribution of LAT GRBs on Rt and t_{90} is presented at figure 5. The investigation results conclude 2 long GRBs subgroup existence separated by limit where maximum energy photon arrival time is equal to event t_{90} . The bursts distribution on high energy episode duration and t_{90} is shown at figure 6. Using this parameter also it is possible to separate two subtypes of GRBs. During first subtype events high energy emission duration interval smaller than t_{90} . Second subtype characterized longer period of high energy emission than t_{90} . But second subtype bursts also divided to 2 subgroups. For one (a) gamma-quantum with maximum energy arrived within t_{90} , and for other (b) such photon was registered later than t_{90} . Such GRBs examples are shown at figure 7.

Furthermore, interval of such emission lasting often so long that mentioned as high energy afterglow, it is not prompt emission. For example, the high energy gamma-emission during of GRB090902 began after more than 100 sec following burst t_{90} end and photon with highest energy $E \sim 9$ GeV was observed more than 50 s later - see figure 8.

Also subTeV emission has characteristics the same than 2b type. MAGIC start registration of GRB190114C about 50 s after the trigger and detected > 300 GeV photons for the first 20 minutes from this burst with a significance higher than 20σ [23]. HESS began observation of GRB 180720B at about 10 h after the burst trigger and detected 100-440 GeV photons at such late time interval [24]. During GRB 160821B MAGIC detected subTeV photons up to 10^4 s after burst trigger [21]. Thus, all observed high-energy photons in subTeV region could be interpreted as afterglow at least for GRB 970417a, GRB190114C, GRB180720B and GRB160821B and subTeV prompt emission was not registered during GRB. GRB160821B is near ($z = 0.16$ [21]) short burst: $t_{90} = 0.48 \pm 0.07$ s in energy region 15-350 keV on Swift/BAT data [25] but $t_{90} \sim 1$ s in energy band 50-300 keV on Fermi/GBM data [26]. GRB190114C and GRB180720B are near ($z = 0.4245$ and $z = 0.653$ correspondingly) long bursts with duration more than 120 s [17,18] and 150 s [27,28] respectively. Redshift measurements provide analyzing additional parameter and at least two long GRBs subgroup were separated with different characteristic distances $z \sim 1.1$ and $z \sim 2.2$. Moreover, preliminary results of analysis allow concluding intermediate GRBs has more high redshift.

3. Conclusion

Firstly GGBs divided only for 2 groups on their duration (short and long). Than subgroup of intermediate events was separated within long events. Redshift measurements allow to analyze additional parameter and at least two long GRBs subgroup again were separated with different characteristic distance. Also for 14 events highest energy gammas detected within t_{90} interval, but for other 41 bursts it registered more than 10 seconds later than one. Moreover, preliminary results of analysis allow to conclude three types of GRBs with high energy emission registration without dependence of burst duration value. During first subtype events high energy emission duration interval smaller than t_{90} . Second subtype subtype characterized longer period of high energy emission than t_{90} . But second subtype bursts divided to 2 subgroups. For one (a) gamma-quantum with maximum energy arrived within t_{90} , and for other such photon was registered later than t_{90} . Therefore, results of preliminary analyses allow conclude long GRBs population inhomogeneity.

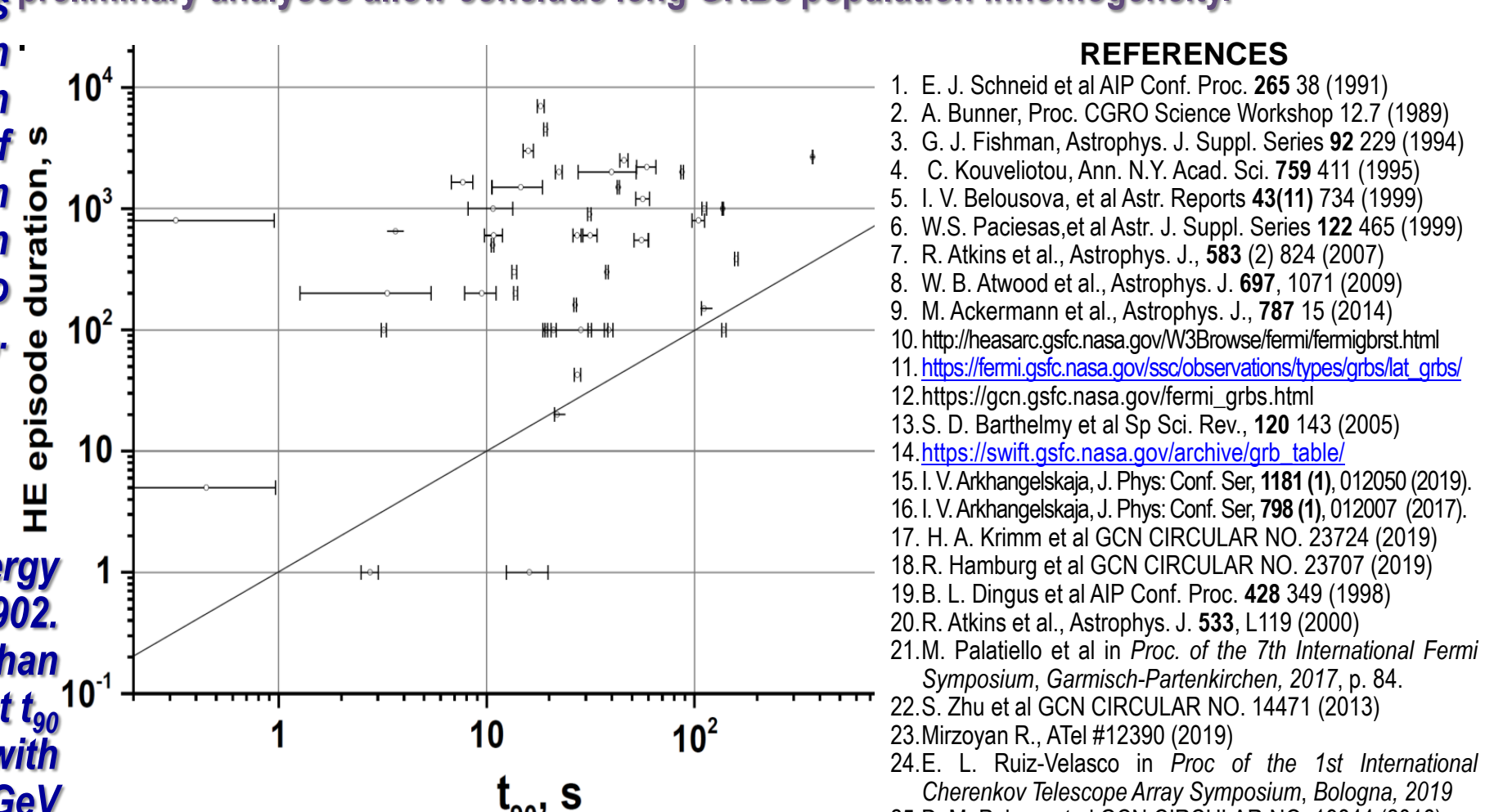


Fig. 6. LAT GRBs distribution on burst HE episode emission duration and t_{90} .

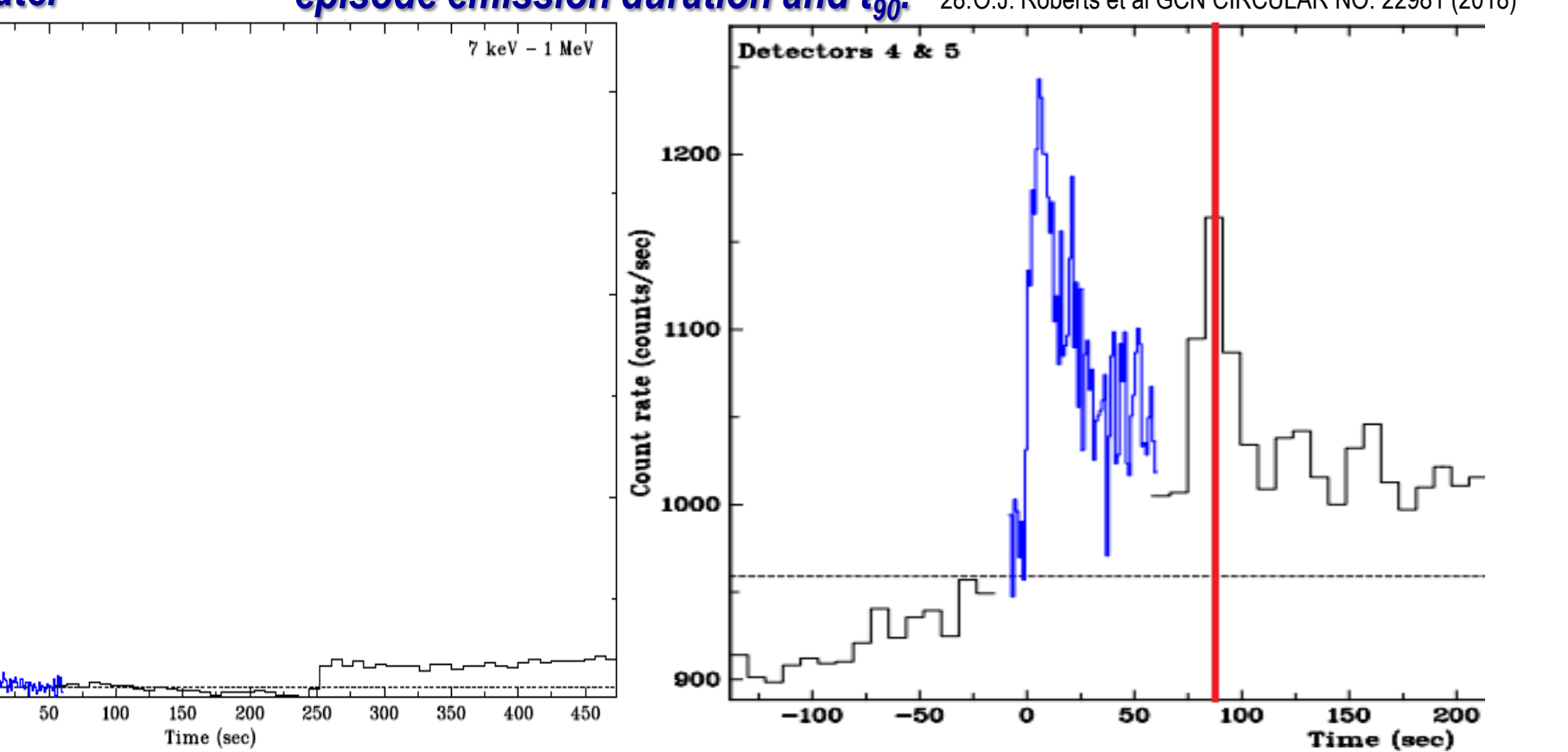


Fig. 8. The high energy afterglow of GRB090902. It began after more than 100 sec following burst t_{90} end and photon with highest energy $E \sim 9$ GeV was observed more than 50 s later

REFERENCES

1. E. J. Schneid et al AIP Conf. Proc. 265 38 (1991)
2. A. Bunner, Proc. CGRO Science Workshop 12.7 (1989)
3. G. J. Fishman, Astrophys. J. Suppl. Series 92 229 (1994)
4. C. Kouveliotou, Ann. N.Y. Acad. Sci. 759 411 (1995)
5. I. V. Belousova, et al Astr. Reports 43(11) 734 (1999)
6. W. S. Paciesas, et al Astr. J. Suppl. Series 122 465 (1999)
7. R. Atkins et al., Astrophys. J., 583 (2) 824 (2007)
8. W. B. Atwood et al., Astrophys. J., 697, 1071 (2009)
9. M. Ackermann et al., Astrophys. J., 787 15 (2014)
10. <http://heasarc.gsfc.nasa.gov/W3Browse/fermi/fermigbrst.html>
11. https://fermi.gsfc.nasa.gov/observations/types/grbslat_grbs/
12. https://gcn.gsfc.nasa.gov/fermi_grbs.html
13. S. D. Barthelmy et al Sp. Sci. Rev., 120 143 (2005)
14. https://swift.gsfc.nasa.gov/archive/grb_table/
15. I. V. Arkhangelskaja, J. Phys. Conf. Ser., 1181 (1), 012050 (2019).
16. I. V. Arkhangelskaja, J. Phys. Conf. Ser., 798 (1), 012007 (2017).
17. H. A. Krimm et al GCN CIRCULAR NO. 23724 (2019)
18. R. Hamburg et al GCN CIRCULAR NO. 23707 (2019)
19. B. L. Dingus et al AIP Conf. Proc. 428 349 (1998)
20. R. Atkins et al., Astrophys. J. 533, L119 (2000)
21. M. Palatiello et al in Proc. of the 7th International Fermi Symposium, Garmisch-Partenkirchen, 2017, p. 84.
22. S. Zhu et al GCN CIRCULAR NO. 14471 (2013)
23. Mirzoyan R., ATel #12390 (2019)
24. E. L. Ruiz-Velasco in Proc of the 1st International Cherenkov Telescope Array Symposium, Bologna, 2019
25. D. M. Palmer et al GCN CIRCULAR NO. 19844 (2016)
26. M. Stanbro et al GCN CIRCULAR NO. 19843 (2016)
27. M. H. Siegel et al GCN CIRCULAR NO. 22973 (2018)
28. O. J. Roberts et al GCN CIRCULAR NO. 22981 (2018)